R_{total} indicates that the centre of curvature has a negative y_2-coordinate.

The results of this work were obtained independently in Munich and Amsterdam.

The authors wish to thank Prof. Dr. H. EWALD and Prof. Dr. J. KISTEMAKER respectively for their stimulating interest.

The work made in Munich was made possible by financial support of the Bundesministerium für Atomkernenergie und Wasserwirtschaft in Bad Godesberg. The work made in Amsterdam is part of the program of research of the Stichting voor Fundamenteel Onderzoek der Materie, and was made possible by financial support of the Nederlandse Organisatie voor Zuiver Wetenschappelijk Onderzoek.

Calculation of the Ion Optical Properties of Inhomogeneous Magnetic Sector Fields
Part 3: Oblique Incidence and Exit at Curved Boundaries

By H. A. TASMAN and A. J. H. BOERBOOM

F.O.M.-Laboratorium voor Massaspectrografie, Amsterdam, Holland,

and H. WACHSMUTH

Physikalisches Institut der Technischen Hochschule, München

(Z. Naturforschg. **14 a**, 822—827 [1959]; eingegangen am 14. Juni 1959)

In previous papers [1, 2] we presented the radial second order imaging properties of inhomogeneous magnetic sector fields with normal incidence and exit at plane boundaries. These fields may provide very high mass resolving power and mass dispersion without increase in radius or decrease of slit widths. In the present paper the calculations are extended to include the effect of oblique incidence and exit at curved boundaries. The influence of the fringing fields on axial focusing when the boundaries are oblique, is accounted for. It is shown that the second order angular aberration may be eliminated by appropriate curvature of the boundaries.

In previous papers (TASMAN and BOERBOOM [1]; WACHSMUTH, BOERBOOM and TASMAN [2]) we calculated the imaging properties of inhomogeneous magnetic sector fields with normal incidence and exit of the main path at plane boundaries. The median plane was supposed to be a plane of symmetry for the magnetic vector potential.

The present paper deals with the most general case if the symmetry with respect to the median plane is retained, i. e. that of curved oblique boundaries. The sector field approximation is retained, i. e. the field strength is supposed to be independent of the path coordinate within the field boundaries where it falls off to zero abruptly. The field boundaries are assumed to consist of lines normal to the median plane. The influence of the fringing fields on axial focusing when the boundaries are oblique, is accounted for.

The coordinate system is identical to that used in the previous paper [2] (Fig. 1). Some of the relevant parameters are shown in Fig. 2. The shape of the boundaries is defined by the projection on the median plane (Fig. 3). The obliqueness at the entrance and exit of the main path is defined by the

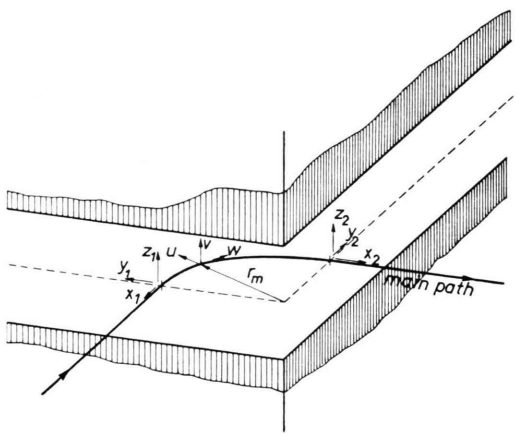

Fig. 1.

angles ε' and ε''. These quantities are positive as shown in Fig. 3. The radii of curvature of the entrance and exit boundaries are R' and R'', which quantities are chosen to be positive if the corresponding boundary is convex towards field-free space. In Fig. 3, both R' and R'' are positive.

[1] H. A. TASMAN and A. J. H. BOERBOOM, Z. Naturforschg. **14 a**, 121 [1959].

[2] H. WACHSMUTH, A. J. H. BOERBOOM and H. A. TASMAN, Z. Naturforschg. **14 a**, 818 [1959].

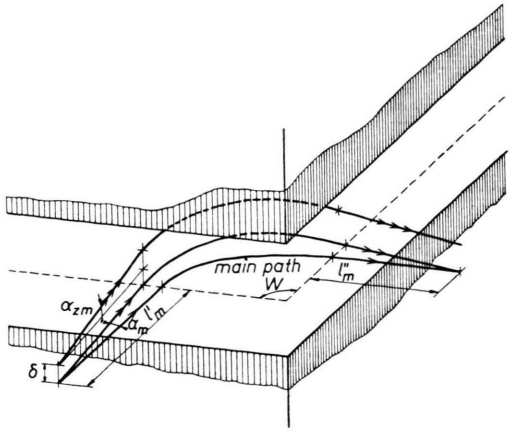

Fig. 2.

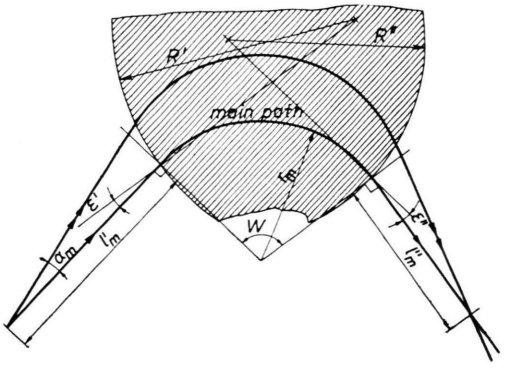

Fig. 3.

The rectilinear paths in the field-free object and image space are supposed to coincide with the tangents to the curved trajectories at the field boundaries. The effect of oblique and/or curved boundaries follows from geometrical considerations. We calculate the second order approximation of the ion trajectories in the image space, related to focusing in radial direction. Axial focusing was treated in first order approximation in the preceeding papers [1, 2]; it remains unaffected by the curvature of boundaries, but is altered by the axial lens action of the fringing fields in case of oblique incidence and exit.

1. Oblique incidence

We will first treat the influence of plane oblique boundaries. The projection on the median plane is represented by Fig. 4.

If u_0, α, v_0, α_z, are the values of u, du/dw, v, dv/dw respectively, at $w=0$ (boundary conditions, see Fig. 1), and if β is related to the momentum-to-charge ratio of the ion through:

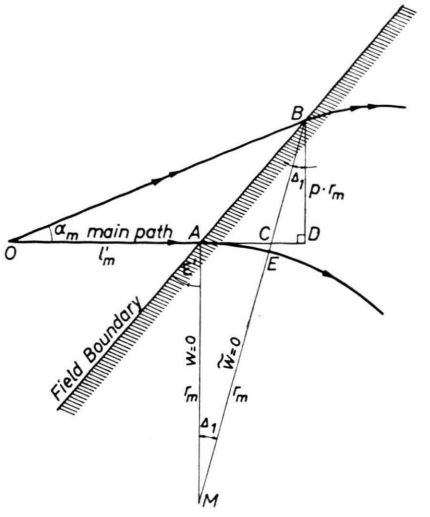

Fig. 4.

$$\frac{m\,v}{e} = \frac{m_0\,v_0}{e_0}\,(1+\beta) \tag{1}$$

it has been derived in the previous papers, that the radial second order approximation of the ion trajectory within the field region may be represented by:

$$\begin{aligned} u = u(w) = {} & D_1\,u_0 + D_2\,\alpha + D_3\,\beta + D_{11}\,u_0^2 + D_{12}\,u_0\,\alpha \\ & + D_{22}\,\alpha^2 + D_{13}\,u_0\,\beta + D_{23}\,\alpha\,\beta + D_{33}\,\beta^2 \\ & + D_{44}\,v_0^2 + D_{45}\,v_0\,\alpha_z + D_{55}\,\alpha_z^2. \end{aligned} \tag{2}$$

For the field shape specified by [23] – [27], [30] – [32] * the quantities D_1, D_2, etc. are given by [37] and {7} **.

In Fig. 4 the main path is OAE. $OA = l_m'$; $MA = ME = r_m$. If the trajectories in the field region are measured in the coordinates u, v, w, (Fig. 1), the origin may still be chosen. In Fig. 4, two such coordinate systems are indicated, differing only in origin. The first system, in which all trajectories should finally be expressed, has its origin $w=0$ at the point of entrance of the main path. The second, rotated system, distinguished by a "~", has $\tilde{w}=0$ at the point of entrance of some other path OB under consideration. If $BD \perp OA$, and designating $BD/r_m = p$, we read from Fig. 4 the relations (omitting terms of third and higher order, and writing $t' = \tan\varepsilon'$):

$$\Delta_1 = \arctan\frac{p\,t'}{p+1} = (p-p^2)\,t' + \ldots, \tag{3}$$

$$\begin{aligned} p = \tan\alpha_m\{(l_m'/r_m) + p\,t'\} = {} & \alpha_m(l_m'/r_m) \\ & + \alpha_m^2(l_m'/r_m)\,t' + \ldots \end{aligned} \tag{4}$$

* Numbers in square brackets [ ] refer to expressions in the previous article [1].

** Numbers in braces { } refer to expressions in the article [2].

and consequently:

$$\Delta_1 = \{\alpha_m (l_m'/r_m) - \alpha_m^2 (l_m'/r_m)^2\}\, t' + \alpha_m^2 (l_m'/r_m)\, t'^2 + \dots . \quad (5)$$

Now $BC = BD/\cos \Delta_1$, and $MC = r_m/\cos \Delta_1$, and thus $\tilde{u}_0$ (measured in the rotated system) equals:

$$\tilde{u}_0 = \frac{BE}{r_m} = \frac{(BD/r_m)+1}{\cos \Delta_1} - 1 = \alpha_m (l_m'/r_m) + \alpha_m^2 (l_m'/r_m)\, t' + \tfrac{1}{2} \alpha_m^2 (l_m'/r_m)^2 t'^2 + \dots . \quad (6)$$

$\tilde{\alpha}$ (measured in the rotated system) equals:

$$\tilde{\alpha} = (\alpha_m + \Delta_1)(1 + \tilde{u}_0) = \alpha_m + \alpha_m^2 (l_m'/r_m) + \alpha_m (l_m'/r_m)\, t' + \alpha_m^2 (l_m'/r_m)\, t'^2 + \dots . \quad (7)$$

The relations

$$\alpha_z = \alpha_{zm} + \alpha_m \alpha_{zm} (l_m'/r_m) + \dots , \quad (8)$$

$$v_0 = (l_m'/r_m)\, \alpha_{zm} + \delta/r_m + \dots \quad (9)$$

are not effected by the oblique entrance in the approximation used. Substitution of (6), (7), (8), and (9) into (2) yields the radial second order approximation in the rotated system. Substituting in this expression:

$$\tilde{w} = w - \Delta_1 \quad (10)$$

and expanding in a TAYLOR series in Δ_1, we obtain the radial second order approximation measured in the fixed coordinate system [with $D_j' = dD_j/dw$]:

$$\begin{aligned} u = u(w) = {} & [D_2 + \{D_1 + D_2 t'\}(l_m'/r_m)]\, \alpha_m + D_3 \beta + [D_{22} + \{D_{12} + D_2 + (D_1 + 2D_{22} - D_2')\, t' \\ & + D_2 t'^2\}(l_m'/r_m) + \{D_{11} + (D_{12} - D_1')\, t' + (\tfrac{1}{2} D_1 + D_{22} - D_2')\, t'^2\}(l_m'/r_m)^2]\, \alpha_m^2 \\ & + [D_{23} + \{D_{13} + (D_{23} - D_3')\, t'\}(l_m'/r_m)]\, \alpha_m \beta + D_{33} \beta^2 \\ & + [D_{55} + D_{45}(l_m'/r_m) + D_{44}(l_m'/r_m)^2]\, \alpha_{zm}^2 + [D_{45} + 2D_{44}(l_m'/r_m)]\, \alpha_{zm} (\delta/r_m) + D_{44} (\delta/r_m)^2 . \end{aligned} \quad (11)$$

2. Oblique exit

The projection on the median plane is represented by Fig. 5. Besides the fixed coordinate system x_2, y_2 (with its origin at the point of exit A of the main path GAI, and with the x_2-axis coinciding with the main path in the image space), a second, rotated coordinate system is indicated, distinguished by a "~".

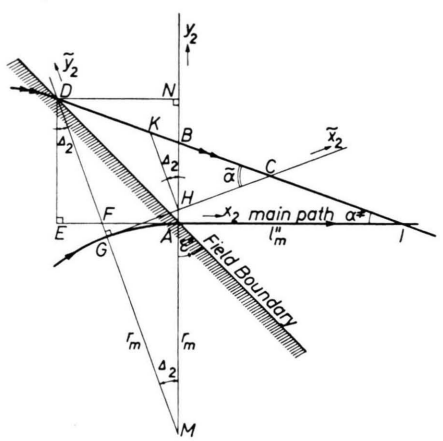

Fig. 5.

The line $\tilde{x}_2 = 0$ of this second system includes the point of exit of some other path DBCI under consideration. $GM = AM = r_m$. Writing $\tilde{U} = DG/r_m$, the path DBCI is presented relative to the rotated system by the equation:

$$\tilde{y}_2 = r_m \tilde{U} - \tilde{x}_2 \tan \tilde{\alpha} . \quad (12)$$

Writing $U^{+} = AB/r_m$, the corresponding expression relative to the fixed coordinate system is

$$y_2 = r_m U^{+} - x_2 \tan \alpha^{+} .$$

We will designate by U, U', U'', the values of u, du/dw, d^2u/dw^2 respectively at $w = W$, irrespective of the limitation of the deflecting field by the field boundary. W is the sector angle (see Fig. 3).

We have:

$$\tilde{U} = U - U' \Delta_2 + \tfrac{1}{2} U'' \Delta_2^2 - \dots . \quad (13)$$

Now $MF = r_m/\cos \Delta_2$; $DE = DF \cos \Delta_2$; $DN = EA = DE \tan \varepsilon'$, and consequently: (writing $t'' = \tan \varepsilon''$) $\Delta_2 = \arcsin(DN/DM)$

$$= U t'' - U^2 t''^2 - U U' t''^2 - \tfrac{1}{2} U^2 t''^3 + \dots , \quad (14)$$

$$\tilde{U} = U - U U' t'' + \dots . \quad (15)$$

We have:

$$\tilde{\alpha} = -\tilde{U}' + \tilde{U}\tilde{U}' + \dots = -U' + U U' + U U'' t'' + \dots . \quad (16)$$

Now $\triangle$ DCG $\sim$ $\triangle$ KCH, and thus

$$KH = r_m (\tilde{U} - \tan \tilde{\alpha} \tan \triangle_2) .$$

As $\triangle$ KBH $\sim$ $\triangle$ DBM, we may deduce:

$$U^{+} = AB/r_m = U + \tfrac{1}{2} U^2 t''^2 + \dots . \quad (17)$$

From Fig. 5, we read:

$$\alpha^{\neq} = \tilde{\alpha} - \triangle_2 = -U' + U\,U' + (-U + U\,U'' + U^2)\,t'' + U\,U'\,t''^2 + \tfrac{1}{2}\,U^2\,t'^3 + \ldots . \quad (18)$$

In (17) – (18), the expression $U = u(W)$ according to (11) should be substituted. It is then found that the radial second order approximation of the path in the image space may be written in the general form:

$$\begin{aligned} y_2 = r_m \{ & M_1\,\alpha_m + M_2\,\beta + M_{11}\,\alpha_m^2 + M_{12}\,\alpha_m\,\beta + M_{22}\,\beta^2 \\ & + M_{33}\,\alpha_{zm}^2 + M_{34}\,\alpha_{zm}(\delta/r_m) + M_{44}(\delta/r_m)^2\} \\ & + x_2\{N_1\,\alpha_m + N_2\,\beta + N_{11}\,\alpha_m^2 + N_{12}\,\alpha_m\,\beta + N_{22}\,\beta^2 \\ & + N_{33}\,\alpha_{zm}^2 + N_{34}\,\alpha_{zm}(\delta/r_m) + N_{44}(\delta/r_m)^2\} . \end{aligned} \quad (19)$$

The coefficients M_i, N_i, may be written as:

$$\left.\begin{aligned} M_1 &= \mu_{1a} + \mu_{1b}(l_m'/r_m), & M_2 &= \mu_{2a}, \\ M_{11} &= \mu_{11a} + \mu_{11b}(l_m'/r_m) + \mu_{11c}(l_m'/r_m)^2, & & \\ M_{12} &= \mu_{12a} + \mu_{12b}(l_m'/r_m), & M_{22} &= -x_2\,\mathrm{tg}\,\alpha \\ M_{33} &= \mu_{33a} + \mu_{33b}(l_m'/r_m) + \mu_{33c}(l_m'/r_m)^2, & & \\ M_{34} &= \mu_{34a} + \mu_{34b}(l_m'/r_m), & M_{44} &= \mu_{44a}; \end{aligned}\right\} \quad (20)$$

$$\left.\begin{aligned} N_1 &= \nu_{1a} + \nu_{1b}(l_m'/r_m), & N_2 &= \nu_{2a}, \\ N_{11} &= \nu_{11a} + \nu_{11b}(l_m'/r_m) + \nu_{11c}(l_m'/r_m)^2. & & \\ N_{12} &= \nu_{12a} + \nu_{12b}(l_m'/r_m), & N_{22} &= \nu_{22a}, \\ N_{33} &= \nu_{33a} + \nu_{33b}(l_m'/r_m) + \nu_{33c}(l_m'/r_m)^2, & & \\ N_{34} &= \nu_{34a} + \nu_{34b}(l_m'/r_m), & N_{44} &= \nu_{44a}. \end{aligned}\right\} \quad (21)$$

The evaluation of the coefficients μ_j, ν_j, will be postponed until after a discussion of the effect of curved boundaries.

3. Curved boundaries

A discussion of the effect of curved boundaries on the coefficients μ_j, ν_j, for a homogeneous magnetic sector field, was presented by KÖNIG and HINTENBERGER [3]. The curvature changes only some of the second order coefficients. The reasoning of KÖNIG and HINTENBERGER applies equally to inhomogeneous magnetic sector fields. If μ_j, ν_j represent the coefficients in (20) – (21) for oblique incidence and exit at curved boundaries with radii of curvature R' and R'' (see Fig. 3) and $\bar{\mu}_j$, $\bar{\nu}_j$ are the corresponding coefficients for normal incidence and exit at plane boundaries, the relation between them may be expressed from the above arguments by: (with

$$t' = \tan\varepsilon'\,;\; t'' = \tan\varepsilon''\,;\; \varrho' = \frac{r_m}{2\,R'\cos^3\varepsilon'}\,;\; \varrho'' = \frac{r_m}{2\,R''\cos^3\varepsilon''}$$

$$\left.\begin{aligned} \mu_{1a} &= \bar{\mu}_{1a}, \quad \mu_{1b} = \bar{\mu}_{1b} + \bar{\mu}_{1a}\,t', \\ \mu_{2a} &= \bar{\mu}_{2a}, \quad \mu_{11a} = \bar{\mu}_{11a} + \tfrac{1}{2}\,\bar{\mu}_{1a}^2\,t''^2, \\ \mu_{11b} &= \bar{\mu}_{11b} + 2\,\bar{\mu}_{11a}\,t' + \bar{\mu}_{1a}\,t'^2 + \bar{\mu}_{1b}\,\bar{\mu}_{1a}\,t''^2 \\ &\quad + \bar{\mu}_{1a}^2\,t'\,t''^2, \\ \mu_{11c} &= \bar{\mu}_{11c} + (\bar{\mu}_{11b} - n\,\bar{\mu}_{1a})\,t' \\ &\quad + (\bar{\mu}_{11a} - \tfrac{1}{2}\,\bar{\mu}_{1b})\,t'^2 + \tfrac{1}{2}\,\bar{\mu}_{1b}^2\,t''^2 \\ &\quad + \bar{\mu}_{1a}\,\bar{\mu}_{1b}\,t'\,t''^2 + \tfrac{1}{2}\,\bar{\mu}_{1a}^2 t'^2\,t''^2 + \varrho'\,\bar{\mu}_{1a}, \\ \mu_{12a} &= \bar{\mu}_{12a} + \bar{\mu}_{1a}\,\bar{\mu}_{2a}\,t''^2, \\ \mu_{12b} &= \bar{\mu}_{12b} + (\bar{\mu}_{12a} - \bar{\mu}_{1a})\,t' + \bar{\mu}_{1b}\,\bar{\mu}_{2a}\,t''^2 \\ &\quad + \bar{\mu}_{1a}\,\bar{\mu}_{2a}\,t'\,t''^2, \\ \mu_{22a} &= \bar{\mu}_{22a} + \tfrac{1}{2}\,\bar{\mu}_{2a}^2\,t''^2, \\ \mu_{33a} &= \bar{\mu}_{33a}, \; \mu_{33b} = \mu_{34a} = \bar{\mu}_{33b}, \\ \mu_{33c} &= \tfrac{1}{2}\,\mu_{34b} = \mu_{44a} = \bar{\mu}_{33c}\,; \end{aligned}\right\} \quad (22)$$

$$\begin{aligned}
\nu_{1a} &= \bar{\nu}_{1a} + \bar{\mu}_{1a}\,t'', \qquad \nu_{1b} = \bar{\nu}_{1b} + \bar{\nu}_{1a}\,t' + \bar{\mu}_{1b}\,t'' + \bar{\mu}_{1a}\,t'\,t'', \qquad \nu_{2a} = \bar{\nu}_{2a} + \bar{\mu}_{2a}\,t'', \\
\nu_{11a} &= \bar{\nu}_{11a} + (\bar{\mu}_{11a} - n\,\bar{\mu}_{1a}^2)\,t'' - \bar{\mu}_{1a}\,\bar{\nu}_{1a}\,t''^2 - \tfrac{1}{2}\,\bar{\mu}_{1a}^2\,t''^3 + \varrho''\,\bar{\mu}_{1a}^2, \\
\nu_{11b} &= \bar{\nu}_{11b} + 2\,\bar{\nu}_{11a}\,t' + (\bar{\mu}_{11b} - 2\,n\,\bar{\mu}_{1a}\,\bar{\mu}_{1b})\,t'' + \bar{\nu}_{1a}\,t'^2 + 2(\bar{\mu}_{11a} - n\,\bar{\mu}_{1a}^2)\,t'\,t'' - (\bar{\mu}_{1a}\,\bar{\nu}_{1b} + \bar{\mu}_{1b}\,\bar{\nu}_{1a})\,t''^2 \\
&\quad - \bar{\mu}_{1a}\,\bar{\mu}_{1b}\,t''^3 - 2\,\bar{\mu}_{1a}\,\bar{\nu}_{1a}t'\,t''^2 + \bar{\mu}_{1a}\,t'^2\,t'' - \bar{\mu}_{1a}^2\,t'\,t''^3 + 2\,\varrho''(\bar{\mu}_{1a}\,\bar{\mu}_{1b} + \bar{\mu}_{1a}^2\,t'), \\
\nu_{11c} &= \bar{\nu}_{11c} + (\bar{\nu}_{11b} - n\,\bar{\nu}_{1a})\,t' + (\bar{\mu}_{11c} - n\,\bar{\mu}_{1b}^2)\,t'' + (\bar{\nu}_{11a} - \tfrac{1}{2}\,\bar{\nu}_{1b})\,t'^2 + (\bar{\mu}_{11a} - n\,\bar{\mu}_{1a}^2 - \tfrac{1}{2}\,\bar{\mu}_{1b})\,t'^2\,t'' \\
&\quad + (\bar{\mu}_{11b} - 2\,n\,\bar{\mu}_{1a}\,\bar{\mu}_{1b} - n\,\bar{\mu}_{1a})\,t'\,t'' - \bar{\mu}_{1b}\,\nu_{1b}t''^2 - (\bar{\mu}_{1a}\,\bar{\nu}_{1b} + \bar{\mu}_{1b}\,\bar{\nu}_{1a})\,t'\,t''^2 - \tfrac{1}{2}\,\bar{\mu}_{1b}^2\,t''^3 \\
&\quad - \bar{\mu}_{1a}\,\bar{\mu}_{1b}\,t'\,t''^3 - \bar{\mu}_{1a}\,\bar{\nu}_{1a}t'^2\,t''^2 - \tfrac{1}{2}\,\bar{\mu}_{1a}^2\,t'^2\,t''^3 + \varrho''(\bar{\mu}_{1b}^2 + 2\,\bar{\mu}_{1a}\,\bar{\mu}_{1b}\,t' + \bar{\mu}_{1a}^2\,t'^2) + \varrho'(\bar{\nu}_{1a} + \bar{\mu}_{1a}\,t''), \\
\nu_{12a} &= \bar{\nu}_{12a} + (\bar{\mu}_{12a} - 2\,n\,\bar{\mu}_{1a}\,\bar{\mu}_{2a} - \bar{\mu}_{1a})\,t'' - (\bar{\mu}_{1a}\,\bar{\nu}_{2a} + \bar{\mu}_{2a}\,\bar{\nu}_{1a})\,t''^2 - \bar{\mu}_{1a}\,\bar{\mu}_{2a}\,t''^3 + 2\,\varrho''\,\bar{\mu}_{1a}\,\bar{\mu}_{2a}, \\
\nu_{12b} &= \bar{\nu}_{12b} + (\bar{\nu}_{12a} - \bar{\nu}_{1a})\,t' + (\bar{\mu}_{12b} - 2\,n\,\bar{\mu}_{1b}\,\bar{\mu}_{2a} - \bar{\mu}_{1b})\,t'' - (\bar{\mu}_{1b}\,\bar{\nu}_{2a} + \bar{\mu}_{2a}\,\bar{\nu}_{1b})\,t''^2 + (\bar{\mu}_{12a} - 2\,n\,\bar{\mu}_{1a}\,\bar{\mu}_{2a} \\
&\quad - 2\,\bar{\mu}_{1a})\,t'\,t'' - \bar{\mu}_{1b}\,\bar{\mu}_{2a}\,t''^3 - (\bar{\mu}_{1a}\,\bar{\nu}_{2a} + \bar{\mu}_{2a}\,\bar{\nu}_{1a})\,t'\,t''^2 - \bar{\mu}_{1a}\,\bar{\mu}_{2a}\,t'\,t''^3 + 2\,\varrho''\,(\bar{\mu}_{1b}\,\bar{\mu}_{2a} + \bar{\mu}_{1a}\,\bar{\mu}_{2a}\,t'), \\
\nu_{22a} &= \bar{\nu}_{22a} + (\bar{\mu}_{22a} - n\,\bar{\mu}_{2a}^2 - \bar{\mu}_{2a})\,t'' - \bar{\mu}_{2a}\,\bar{\nu}_{2a}\,t''^2 - \tfrac{1}{2}\,\bar{\mu}_{2a}^2\,t''^3 + \varrho''\,\bar{\mu}_{2a}^2, \\
\nu_{33a} &= \bar{\nu}_{33a} + \bar{\mu}_{33a}\,t'', \qquad \nu_{33b} = \nu_{34a} = \bar{\nu}_{33b} + \bar{\mu}_{33b}\,t'', \qquad \nu_{33c} = \tfrac{1}{2}\,\nu_{34b} = \nu_{44a} = \bar{\nu}_{33c} + \bar{\mu}_{33c}\,t''\,.
\end{aligned} \quad (23)$$

For reference, the coefficients $\bar{\mu}_j$, $\bar{\nu}_j$, for normal incidence and exit at plane boundaries are summarised

[3] L. A. KÖNIG and H. HINTENBERGER, Z. Naturforschg. **12 a**, 377 [1957].

below:

$$
\begin{aligned}
&\bar{\mu}_{1a} = (1-n)^{-1/2}\sin W^*, \quad \bar{\mu}_{1b} = \cos W^*, \quad \bar{\mu}_{2a} = (1-n)^{-1}(1-\cos W^*),\\
&\bar{\mu}_{11a} = \tfrac{1}{6}(1-n)^{-1}\{(X-3)\cos^2 W^* - (2X-3)\cos W^* + X\},\\
&\bar{\mu}_{11b} = \tfrac{1}{3}(1-n)^{-1/2}\{X\sin W^* - (X-3)\sin W^*\cos W^*\},\\
&\bar{\mu}_{11c} = \tfrac{1}{6}\{X(1-\cos W^*) + (X-3)\sin^2 W^*\},\\
&\bar{\mu}_{12a} = \tfrac{1}{6}(1-n)^{-3/2}\{2(X-3)\sin W^*\cos W^* + (X-3n+6)\sin W^* - 3(X-n)\,W^*\cos W^*\},\\
&\bar{\mu}_{12b} = \tfrac{1}{6}(1-n)^{-1}\{-2(X-3)\sin^2 W^* - 2X(1-\cos W^*) + 3(X-n)\,W^*\sin W^*\},\\
&\bar{\mu}_{22a} = \tfrac{1}{6}(1-n)^{-2}\{(X-3)\sin^2 W^* + 4X(1-\cos W^*) - 3(X-n)\,W^*\sin W^*\},\\
&\bar{\mu}_{33a} = -\tfrac{1}{4}n^{-1}(1-5n)^{-1}\{\langle 2n - X(1-n)\rangle\cos 2W^\dagger - 2n(1-2X)\cos W^* + X(1-5n)\},\\
&\bar{\mu}_{33b} = \bar{\mu}_{34a} = \tfrac{1}{2}(1-5n)^{-1}n^{-1/2}(1-n)^{-1/2}\langle 2n - X(1-n)\rangle\{(1-n)^{1/2}\sin 2W^\dagger - 2n^{1/2}\sin W^*\},\\
&\bar{\mu}_{33c} = \tfrac{1}{2}\bar{\mu}_{34b} = \bar{\mu}_{44a} = \tfrac{1}{4}(1-5n)^{-1}\{\langle 2n - X(1-n)\rangle\cos 2W^\dagger - 2\langle n - X(1-3n)\rangle\cos W^* - X(1-5n)\}.
\end{aligned}
\tag{24}
$$

$$
\begin{aligned}
&\bar{\nu}_{1a} = \cos W^*, \quad \bar{\nu}_{1b} = -(1-n)^{1/2}\sin W^*, \quad \bar{\nu}_{2a} = (1-n)^{-1/2}\sin W^*,\\
&\bar{\nu}_{11a} = \tfrac{1}{6}(1-n)^{-1/2}\{-2X\sin W^*\cos W^* + (2X-3)\sin W^*\},\\
&\bar{\nu}_{11b} = \tfrac{1}{3}X\{2\sin^2 W^* + \cos W^* - 1\},\\
&\bar{\nu}_{11c} = \tfrac{1}{6}(1-n)^{1/2}X\{2\sin W^*\cos W^* + \sin W^*\},\\
&\bar{\nu}_{12a} = \tfrac{1}{6}(1-n)^{-1}\{-4X\sin^2 W^* + 2X(1-\cos W^*) + 3(X-n)\,W^*\sin W^*\},\\
&\bar{\nu}_{12b} = \tfrac{1}{6}(1-n)^{-1/2}\{-4X\sin W^*\cos W^* + (X-3n+6)\sin W^* + 3(X-n)\,W^*\cos W^*\},\\
&\bar{\nu}_{22a} = \tfrac{1}{6}(1-n)^{-3/2}\{2X\sin W^*\cos W^* + (X+3n-6)\sin W^* - 3(X-n)\,W^*\cos W^*\},\\
&\bar{\nu}_{33a} = \tfrac{1}{2}n^{-1}(1-5n)^{-1}\{n^{1/2}\langle 2n - X(1-n)\rangle\sin 2W^\dagger + (1-n)^{1/2}n(2X-1)\sin W^*\},\\
&\bar{\nu}_{33b} = \bar{\nu}_{34a} = (1-5n)^{-1}\langle 2n - X(1-n)\rangle(\cos 2W^\dagger - \cos W^*),\\
&\bar{\nu}_{33c} = \tfrac{1}{2}\bar{\nu}_{34b} = \bar{\nu}_{44a} = \tfrac{1}{2}(1-5n)^{-1}\{-\langle 2n - X(1-n)\rangle n^{1/2}\sin 2W^\dagger + \langle n - X(1-3n)\rangle(1-n)^{1/2}\sin W^*\}.
\end{aligned}
\tag{25}
$$

The axial component of the trajectory in the image space is still given in first order by:

$$z_2 = r_m\{\Sigma_3\,\alpha_{zm} + \Sigma_4(\delta/r_m)\} + x_2\{T_3\,\alpha_{zm} + T_4(\delta/r_m)\}. \tag{26}$$

$$\Sigma_3 = \sigma_{3a} + \sigma_{3b}(l_m'/r_m), \quad \Sigma_4 = \sigma_{4a}; \tag{27}$$

$$T_3 = \tau_{3a} + \tau_{3b}(l_m'/r_m), \quad T_4 = \tau_{4a}; \tag{28}$$

where the coefficients σ_j, τ_j for normal incidence and exit at plain or curved boundaries are equal to: (with $W^\dagger = n^{1/2}W$)

$$\sigma_{3a} = n^{-1/2}\sin W^\dagger, \quad \sigma_{3b} = \sigma_{4a} = \tau_{3a} = \cos W^\dagger, \quad \tau_{3b} = \tau_{4a} = -n^{1/2}\sin W^\dagger. \tag{29}$$

In case of oblique incidence and exit the stray fields have to be taken into account (Herzog [4]). They act as thin lenses on the entrance and exit side with the focal lengths f_{str}' and f_{str}'' respectively, given by:

$$f_{str}' = r_m\cot\varepsilon', \quad f_{str}'' = r_m\cot\varepsilon''. \tag{30}$$

[4] R. F. K. Herzog, Acta Phys., Austr. **4**, 431 [1950–1951].

(30) is valid independent of the shape of the fringing fields provided that their extension is short compared with f_{str}' or f_{str}''. Thus including the effect of the fringing fields, the coefficients σ_j, τ_j, for oblique incidence and exit at plain or curved boundaries are given by: (with $W^\dagger = n^{1/2}W$; $t' = \tan\varepsilon'$; $t'' = \tan\varepsilon''$)

$$
\begin{aligned}
&\sigma_{3a} = n^{-1/2}\sin W^\dagger;\\
&\sigma_{3b} = \sigma_{4a} = \cos W^\dagger + n^{-1/2}\sin W^\dagger\,t';\\
&\tau_{3a} = \cos W^\dagger + n^{-1/2}\sin W^\dagger\,t'';\\
&\tau_{3b} = \tau_{4a} = -n^{1/2}\sin W^\dagger + \cos W^\dagger(t'+t'')\\
&\quad + n^{-1/2}\sin W^\dagger\,t'\,t''.
\end{aligned}
\tag{31}
$$

For $n = X = 0$ (homogeneous magnetic sector field) the coefficients μ_j; ν_j; (24) – (25) become identical to those presented by König and Hintenberger [3] for this case.

4. Imaging properties of inhomogeneous magnetic sector fields with oblique incidence and exit at curved boundaries

From the reasoning applied in our first paper [1] it follows, that first order directional focusing in

radial direction occurs at the image distance:

$$l_m'' = -r_m M_1/N_1 . \tag{32}$$

This may be expressed in the familiar form:

$$(l_m' - g')(l_m'' - g'') = f^2 . \tag{33}$$

where:

$$\frac{g'}{r_m} = \frac{(1-n)^{1/2}\cos W^* + \sin W^* \tan \varepsilon''}{(1-n)\sin W^* - (1-n)^{1/2}\cos W^*(\tan \varepsilon' + \tan \varepsilon'') - \sin W^* \tan \varepsilon' \tan \varepsilon''} , \tag{34}$$

$$\frac{g''}{r_m} = \frac{(1-n)^{1/2}\cos W^* + \sin W^* \tan \varepsilon'}{(1-n)\sin W^* - (1-n)^{1/2}\cos W^*(\tan \varepsilon' + \tan \varepsilon'') - \sin W^* \tan \varepsilon' \tan \varepsilon''} , \tag{35}$$

$$\frac{f}{r_m} = \frac{1}{(1-n)^{1/2}\sin W^* - \cos W^*(\tan \varepsilon' + \tan \varepsilon'') - (1-n)^{-1/2}\sin W^* \tan \varepsilon' \tan \varepsilon''} . \tag{36}$$

First order directional focusing in axial direction occurs at the axial image distance:

$$l_{zm}'' = -r_m \Sigma_3/T_3 . \tag{37}$$

This may be expressed in the form:

$$(l_m' - g_z')(l_{zm}'' - g_z'') = f_z^2 . \tag{38}$$

Including the effect of the fringing fields the quantities g_z', g_z'', and f_z are given by:

$$\frac{g_z'}{r_m} = \frac{n^{1/2}\cos W^\dagger + \sin W^\dagger \tan \varepsilon''}{n\sin W^\dagger - n^{1/2}\cos W^\dagger(\tan \varepsilon' + \tan \varepsilon'') - \sin W^\dagger \tan \varepsilon' \tan \varepsilon''} , \tag{39}$$

$$\frac{g_z''}{r_m} = \frac{n^{1/2}\cos W^\dagger + \sin W^\dagger \tan \varepsilon'}{n\sin W^\dagger - n^{1/2}\cos W^\dagger(\tan \varepsilon' + \tan \varepsilon'') - \sin W^\dagger \tan \varepsilon' \tan \varepsilon''} , \tag{40}$$

$$\frac{f_z}{r_m} = \frac{1}{n^{1/2}\sin W^\dagger - \cos W^\dagger(\tan \varepsilon' + \tan \varepsilon'') - n^{-1/2}\sin W^\dagger \tan \varepsilon' \tan \varepsilon''} . \tag{41}$$

In a symmetrical arrangement (where $R' = R'' = R$; $\varepsilon' = \varepsilon'' = \varepsilon$; $l_m' = l_m''$) the radial object and image distance are equal to:

$$l_m' = l_m'' = \frac{r_m}{(1-n)^{1/2}\tan(W^*/2) - \tan \varepsilon} . \tag{42}$$

The mass dispersion per unit $\delta m/m_0$ in the y_2-direction for a monoenergetic ion beam, at the image distance l_m'' equals in a symmetrical arrangement

$$D_m = \frac{r_m}{\{1-(1-n)^{-1/2}\cot(W^*/2)\tan \varepsilon\}(1-n)} . \tag{43}$$

The general formulae for the second order aberrations [55], and $\{20\} - \{24\}$ remain valid. Oblique incidence and/or exit affects both the first order and the second order focusing properties, whereas curvature of the boundaries influences only the second order properties. In particular, in a symmetrical arrangement, the second order angular aberration causes image broadening by the amount:

$$A_{11}\alpha_m^2 = \frac{r_m}{1-n}\left\{\frac{\cos W^* + 5}{3(1-\cos W^*)} X + \frac{\cot^3(W^*/2)}{(1-n)^{1/2}}\frac{r_m}{R} - 1\right\}\alpha_m^2 . \tag{44}$$

Provided that $\cot(W^*/2) \neq 0$, (or $W^* \neq \pi$), the second order angular aberration can obviously by eliminated by a proper choice of r_m/R.

The results of this work were obtained independently in Amsterdam and Munich.

The authors wish to thank Prof. Dr. J. KISTEMAKER and Prof. Dr. H. EWALD respectively for their stimulating interest.

The work made in Amsterdam is part of the program of research of the Stichting voor Fundamenteel Onderzoek der Materie, and was made possible by financial support of the Nederlandse Organisatie voor Zuiver Wetenschappelijk Onderzoek. The work made in Munich was made possible by financial support of the Bundesministerium für Atomkernenergie und Wasserwirtschaft in Bad Godesberg.